Vol. 18, No. 2 (2019) 431-439
Revista Mexicana de Ingeniería Química

INDUCED ELECTROCHEMICAL REDUCTION OF NITRATES SPECIES ON INTERFACE OF Pt/MWCNTs PREPARED BY VAPOR-PHASE IMPREGNATION-DECOMPOSITION METHOD

INDUCCIÓN A LA REDUCCION ELECTROQUÍMICA DE ESPECIES NITRADAS SOBRE LA SUPERFICIE DE Pt/MWCNTs PREPARADAS POR EL MÉTODO DE IMPREGACIÓN-DECOMPOSICIÓN EN FASE VAPOR

E. Torres-Santillan[1]*, J. R. Vargas-Garcia[2], E. Ramirez-Meneses[3], A. Manzo-Robledo[1], M. A. Hernandez-Perez[2]

[1]*Instituto Politécnico Nacional, Departamento de Ingeniería Química Industrial, ESIQIE, UPALM Edif. 7, Zacatenco, CP. 07738, CDMX, México.*

[2]*Instituto Politécnico Nacional, Departamento de Metalurgia y Materiales, ESIQIE, UPALM, Zacatenco, CP. 07738, CDMX, México.*

[3]*Universidad Iberoamericana, Departamento de Ingeniería y Ciencias Químicas, Prolongación Paseo de la Reforma 880, C.P. 01219 CDMX, Mexico.*

Received: June 9, 2018; Accepted: October 20, 2018

Abstract

Pt nanoparticles were supported on multi-wall carbon nanotubes (MWCNTs) and conventional C-Vulcan XC72 by a vapor-phase impregnation-decomposition method using platinum acetylacetonate as precursor. Both types of carbon supports were impregnated with the precursor vapors at 180 ºC and 3-7 Torr inside a horizontal quartz tube reactor. Then, they were heated at 400 ºC to achieve precursor decomposition and subsequent formation of Pt nanoparticles. Carbon supports, and Pt precursor were mixed in several weight ratios. The Pt content was approximately 5, 10 and 25 wt.%. TEM observations revealed Pt particles ranging from 2.4 to 3.3 nm uniformly distributed on either nanotubes or conventional carbon support. The catalytic activity for nitrate electro-reduction (NER) was investigated in $NaNO_3$ + NaOH solutions using Cycling Voltammetry (CV). The CV measurements showed a redox process from -0.7 to -1.0 V/SCE associated to the nitrate reduction process. It was found that Pt/MWCNTs materials display superior nitrate reduction activity than Pt/C-Vulcan XC72, even the comparable Pt decisive features. The superior activity seems to be associated to the inherent structural features of MWCNTs. Thus, Pt/MWCNTs are attractive materials for electrodes on the nitrate reduction process in alkaline medium aqueous.

Keywords: Nanoparticles, platinum, carbon nanotubes, electroreduction, nitrates.

Resumen

Nanopartículas de Pt fueron soportadas en nanotubos de carbono de paredes múltiples (MWCNTs) y carbón convencional C-Vulcan XC72 mediante un método de impregnación-descomposición en fase de vapor utilizando acetilacetonato de platino como precursor. Ambos tipos de soportes de carbono se impregnaron con los vapores precursores a 180 °C y 3-7 Torr dentro de un reactor de tubo de cuarzo horizontal. A continuación, se calentaron a 400 °C para lograr la descomposición del precursor y la formación subsiguiente de nanopartículas de Pt. Los soportes de carbono y el precursor de Pt se mezclaron en varias proporciones en peso. El contenido era de aproximadamente 5, 10 y 25% en peso. Las observaciones TEM revelaron partículas de Pt de 2.4 a 3.3 nm uniformemente distribuidas en los nanotubos o soporte de carbono convencional. La actividad catalítica para la electro-reducción de nitratos (ERN) se investigó en soluciones de $NaNO_3$ + NaOH utilizando Voltamperometría Cíclica (VC). Las medidas de VC mostraron un proceso redox de -0.7 a -1.0 V/SCE asociado al proceso de reducción de nitratos. Se encontró que los materiales Pt/MWCNTs muestran una actividad de reducción de nitratos superior a Pt/C-Vulcan XC72, incluso en las características comparables de Pt. La actividad superior parece estar asociada con las características estructurales inherentes de los MWCNTs. Por lo tanto, Pt/MWCNTs es un material atractivo para electrodos en el proceso de reducción de nitratos en medio acuoso alcalino.

Palabras clave: Nanopartículas, platino, nanotubos de carbón, electroreducción, nitratos.

* *Corresponding author. E-mail*: esthersantillan@gmail.com
https://doi.org/10.24275/uam/izt/dcbi/revmexingquim/2019v18n2/Torres
issn-e: 2395-8472

1 Introduction

Nitrate pollution is a common and serious health problem around the world. For several decades, numerous worldwide regions have suffered an increasingly nitrate concentration in groundwater, rivers, lakes and coastal waters. The main sources of nitrate include industrial waste, chemical fertilizers, animal feces and human wastes (Luk *et al*., 2002; Martínez *et al*., 2017). The presence of nitrate in drinking water represents an elevated risk of serious human diseases. The World Health Organization recommends a maximum limit of 50 mgL^{-1} for nitrate concentration in drinking water (Xiaomeng *et al*., 2009). Thus, for long time the neutralization of nitrate in water sources has been a crucial issue of scientific research (Fanning 2000, Park *et al*., 2005; Patel *et al*., 2008). Different methods have been proposed and used commonly for the remediation of drinking water sources such as ion exchange and reverse osmosis (Schoeman *et al*., 2003; Wang *et al*., 2007), however, such processes are relatively costly with derivations in other problems due to their use, (Lehman *et al*., 2008; Martinez *et al*., 2017).

Biological denitrification is also another alternative for remediation of water sources, but the use of microorganisms is unattractive (Park *et al*., 2005). Photocatalysis has been used for the removal of nitrite oxide ions (Toma *et al*., 2006). One important denitrification method is the selective catalytic or electrocatalytic reduction of nitrates offering greater advantages, due to the selectivity, versatility, high energy, low costs and safety, from an environmental point of view, since it is not necessary to add any chemical solution to the effluents used, with the desirable objective of obtaining N_2 as main product and ammonium undesired by-product in alkaline media (Groot *et al*., 2004; Couto *et al*., 2016; Hernández-Fydrych *et al*., 2018). Metal active catalysts such as Pt, Sn, Pd and Cu supported on graphite, carbon Vulcan, TiO_2 and ZrO_2 have been investigated for nitrate electroreduction (Prusse *et al*., 2000; Kerkeni *et al*., 2002; Wang *et al*., 2006; Bhatnagar *et al*., 2010; Bahman *et al*., 2011). In recent years, however, carbon nanotubes (CNTs) have been investigated as support materials for the fabrication of electrocatalysts due to their high surface area, high electrical conductivity and extraordinary thermal stability (Baughman, *et al*., 2002; Serp *et al*., 2003).

Conventional wet impregnation or precipitation methods have been frequently used to incorporate the catalytic active phase on CNTs (Cheng et. al. 2008; Trépanier *et al*., 2009, Soares *et al*., 2011; Torres-Santillan *et al*., 2018). However, methods on gaseous phase such as chemical vapor deposition or vapor-phase impregnation-decomposition (Capula *et al*., 2009, Encarnacion *et al*., 2010; Mercado-Zuñiga *et al*., 2014) allow the incorporation of active nanoparticles on fine-divided porous supports without the need of liquid solvents and their drying and reduction steps, which may promote undesirable changes of active particle size (Vahlas *et al*., 2006). In the present study, we report the incorporation of Pt nanoparticles on MWCNTs by vapor-phase impregnation-decomposition method and their electrocatalytic activity on NER process in alkaline conditions; finally, it is important to compare the performance of Pt nanoparticles synthesis by the same method on C-Vulcan XC72 commercial support at the same conditions.

2 Materials and methods

2.1 *Preparation of Pt/MWCNTs and Pt/C-Vulcan XC72*

Pt nanoparticles were supported on commercial MWCNTs (Aldrich, 6-13 nm in diameter and 2.5-20 μm in length) or C-Vulcan XC72 by a vapor-phase impregnation-decomposition method. MWCNTs and Pt precursor were mixed in 10:1, 4:1, 2:1 weight ratios before vapor-phase impregnation. C-Vulcan and Pt precursor were mixed in 2:1 weight ratio. The mixed powders were heated at 180 ºC for 10 min to evaporate the precursor in a horizontal quartz tube reactor at a total pressure of 3-7 Torr. Then, the impregnated carbon supports were moved to a higher temperature zone (400 ºC) inside the tube reactor to achieve the precursor decomposition under an argon gas flow (FRAr =100 cm^3/min). The crystal structure, particle size and morphology were analyzed by X-ray diffraction (XRD, D8 focus Brucker using Cu-Kα radiation) and electron microscopies (SEM-JEOL 6300 coupled with an EDS detector and MET-FEI TITAN). Pt content in carbon support was determined by atomic adsorption spectroscopy (AAS) with a Perkin-Elmer 2380 apparatus.

2.2 Electrochemical measurements

Electrochemical measurements were performed using a potentiostat/galvanostat (PGSTAT30-2, AUTOLAB) and a conventional three-electrode electrochemical cell. A standard calomel electrode (SCE) and a glassy carbon (GC) rod were employed as reference and counter electrodes, respectively. The working electrodes were prepared by mixing ultrasonically 4 mg of either Pt/MWCNTs or Pt/C-Vulcan, 200 μL of Nafion solution (Aldrich, 5 wt.%) and 1 mL of distilled water. An enough this mixture (4 μL) was uniformly applied over the freshly polished cross-section (0.125 cm^2) of a GC rod and dried by an argon flow for 30 min. Firstly, the working electrodes were activated by cyclic voltammetry (CV) in a 0.5 M H_2SO_4 solution at 50 mVs^{-1}until subsequent changes in the CV curve shape became negligible. Then, the electrocatalytic activity for nitrate electroreduction (NER) was investigated in $NaNO_3$ solutions at a scan rate of 5 $mVs^{-1}$and a potential window from 0.2 to -1.0 V/SCE. The nitrate concentration [NO^{3-}] was varied from 0.001 to 1.0 M in presence of 0.5 M NaOH as supporting electrolyte. Before measurements, the nitrate solution was deaerated by bubbling high purity Argon for 30 min.

3 Results and discussion

The Pt content determined by AAS was approximately 5, 10 and 25 wt.% for 10:1, 4:1, 2:1 and carbon support and Pt precursor weight ratios, respectively.

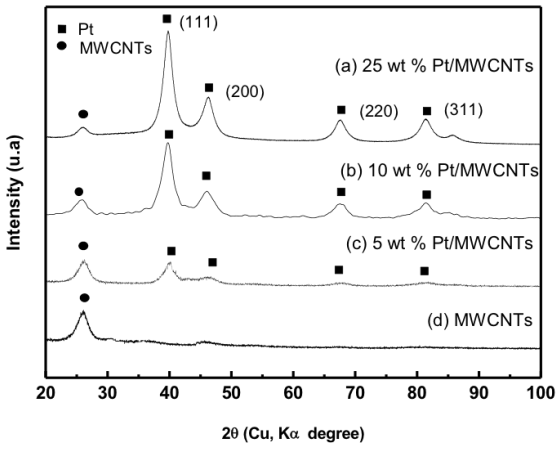

Fig. 1. XRD patterns of (a) MWCNTs, (b) Pt_5/MWCNTs, (c) Pt_{10}/MWCNTs and (d) Pt_{25}/MWCNTs.

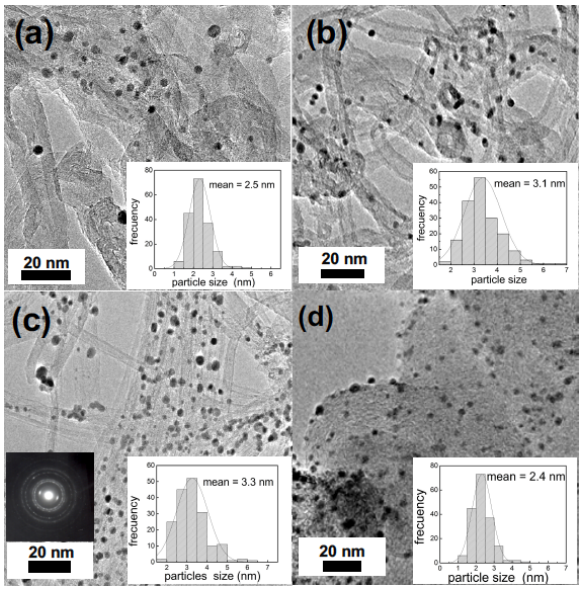

Fig. 2. TEM images of (a) Pt_5/MWCNTs, (b) Pt_{10}/MWCNTs, (c) Pt_{25}/MWCNTs (insert Laue pattern) and (d) Pt_{25}/C-Vulcan.

Fig. 1 shows the typical XRD patterns of (a) MWCTNs, (b) Pt_5/MWCNTs, (c) Pt_{10}/MWCNTs and (d) Pt_{25}/MWCNTs. The angular Bragg positions of Pt (JCPDS 04-0802) are indicated as a reference. The broad reflection at 2θ = 26.3º in Fig. 1(a) has been usually assigned to the (002) plane of the graphite-like structure of MWCNTs (Halder *et al.*, 2009). The gradual increment of the characteristic and broad Pt reflections observed from Figs. 1(b) to 1(d) suggests a progressive increase of small metallic crystallites on the MWCNTs surface. The patterns reflections indicate there is no fundamental change in the MWCNTs structure due to the incorporation of Pt. The conventional C-Vulcan material displayed an amorphous-like nature (not shown here).

Fig. 2 depicts the bright field TEM images of Pt_5/MWCNTs, Pt_{10}/MWCNTs, Pt_{25}/MWCNTs and Pt_{25}/C-Vulcan. These images reveal fine particles in dark contrast, uniformly distributed on either tubular or granular carbon morphology. Since dark contrast might be generated by the high absorption of electrons from heavy atoms in the sample, dark areas were associated with Pt atoms. Statistical analysis indicated that Pt nanoparticles have sizes of about 2.5, 3.1, and 3.3 nm for 5, 10 and 25 wt.% Pt, respectively. For 25 wt.% Pt content, the particle size on C-Vulcan was about 2.4 nm. A narrow size distribution was observed in each case.

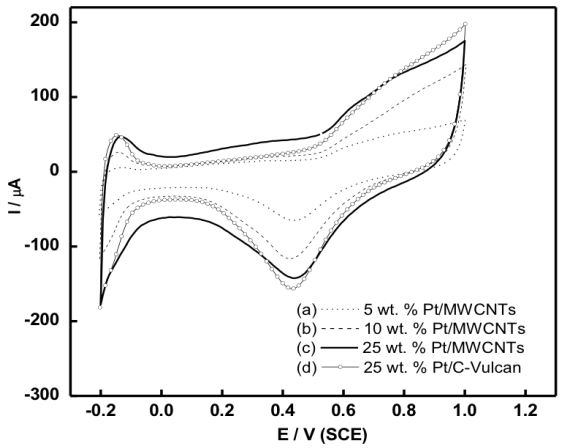

Fig. 3. CVs for Pt/MWCNTs and Pt/C-Vulcan in 0.5 M H_2SO_4 solution at 50 mVs^{-1} and a potential window from -0.2 to 1.0 V/SCE.

The Laue diffraction pattern produced by 200kV and a distance L=100 cm of the sample of Pt_{25}/MWCNTs is shown as an insert in Fig. 2(c). The above results indicate that the particle size of the Pt is not substantially increased, and a high dispersion is maintained even when the metal load increases up to 25% weight. Other methods of incorporating metal particles on carbon supports via wet impregnation have reported agglomeration problems even for minor metallic fillers to 10% (Kijima *et al*., 2004; Abbasi *et al*., 2013; Shenga *et al*., 2014). This suggests that vapor-phase impregnation-decomposition method technique is a factor that favors high dispersion with small Pt particle size. Further investigation by infrared spectroscopy could confirm the functionalization of carbon substrate promoted by the impregnation method in vapor-phase.

Table 1. Included values for BET surface area of Pt/MWCNTs as well as Pt_{25}/C-Vulcan, it can be observed that the Pt/MWCNTs materials exhibit greater surface area than the reference material.

Table 1. BET area for Pt/MWCNTs and Pt_{25}/C-Vulcan

Electrocatalyst	BET area $[m^2g^{-1}]$*
Pt_5/MWCNTs	236.8
Pt_{10}/MWCNTs	257.4
Pt_{25}/MWCNTs	269.1
Pt_{25}/C-Vulcan	201.0

The CV curves for hydrogen and oxygen electro-adsorption on Pt/MWCNTs and Pt/C-Vulcan in a 0.5 M H_2SO_4 solution are shown in Fig. 3. Typical regions of hydrogen adsorption/desorption, double layer and oxygen electro-adsorption on Pt are clearly distinguished at characteristic potentials. Surface redox waves became more intense as Pt content increased. For better comparison of the curves, the electrochemically active surface area (ECSA) in the hydrogen adsorption-desorption zone was calculated per the eq. (1):

$$ECSA = Q_H / Q_{Pt} \quad (1)$$

where Q_H is the charge exchanged during the electro-adsorption of H_2 on Pt/MWCNTs (from -0.2 to 1 V/SCE) and Q_{Pt} = 210 μCcm^{-2} (Lim *et al*., 2009). The Q_H and ECSA values are summarized in the Table 2 and ESCA decreased in the order Pt_{25}/MWCNTs > Pt_{25}/C-Vulcan > Pt_{10}/MWCNTs > Pt_5/MWCNTs.

The ESCA of an electrocatalyst not only determines the number of catalytically active sites available for an electrochemical reaction, but also is an important parameter to compare different supports (Halder *et al*., 2009; Shenga *et al*., 2014). Fig. 4 shows the effects of Pt loading on the cyclic voltammograms of both Pt supported on MWCNTs (a-c) and Pt supported on conventional C-Vulcan (d) in 1M $NaNO_3$ + 0.5 M NaOH solutions. The two types of materials exhibit CV curves having a consistent redox process from -0.7 to -1.0 V/SCE. The maximum current (i_p) associated to this reduction process at about -0.82 V/SCE increases with Pt loading (Manzo-Robledo *et al*., 2007; Estudillo-Wong *et al*., 2011).

This current is clearly attributed to the reduction of nitrate ions since no redox process is observed in the absence of nitrate (insert (e) Fig. 4). A new reduction peak (i_a) appear in the positive scan, due to nitrate reduction on the “fresh" surface sites produced by hydrogen desorption, and the magnitude intensity becomes higher as a function of Pt loading. Electroreduction of nitrates starts in the double-layer region and is characterized by a current maximum at -0.82 V/SCE for both directions of the scan. However, it must be kept in mind that the current is the sum of two processes, the reduction of nitrate ions and the hydrogen adsorption-desorption (Taguchi *et al*., 2008). In a positive scan, also appears a peak (i_b) that can be attributed to the oxidation process of the reduction of nitrates that were carried out in the negative scan and its magnitude becomes greater to higher contents of Pt (Estudillo-Wong *et al*., 2008).

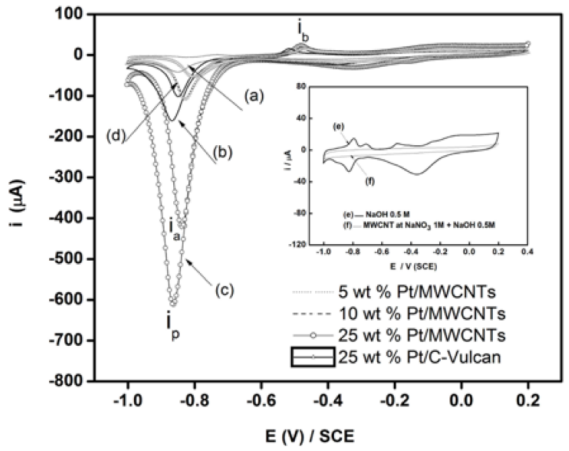

Fig. 4. CVs for Pt/MWCNTs (a) to (c) and conventional Pt_{25}/C-Vulcan (d) in nitrate solutions 1.0 M in alkali medium at 5mVs-1. Insert (e) Pt_{25}/MWCNT in NaOH. Insert (f) MWCNTs in NaNO3 1M + NaOH.

The Pt/MWCNTs display i_p values comparatively higher than those observed with Pt/C-Vulcan, even though the materials have similar ECSA, particle size, Pt distribution and Pt content (for 25 wt.%). Higher NER activity of Pt/MWCNTs seems to be strongly dependent on the inherent structural and electronic features of MWCNTs. The structural features of MWCNTs may facilitate remarkably the electron transfer at the interfacial region between Pt and electrolyte, as no reduction of nitrate is observed on bare MWCNTs (insert (f) Fig. 4). This results in highly catalytic electrodes for the NER process in alkaline medium.

The applied potential and the pH are two elements that play an important role in the NER process whose quantitative determination of products and by-products requires complicated quantitative analytical methods (Brylev *et al*., 2007).

Table 2. Adsorption-desorption charge (Q_H) and ECSA for Pt/MWCNTs and Pt/C-Vulcan

Material	Q_H [μC]	*ECSA [cm^2]
Pt_5/MWCNTs	191.1	0.8
Pt_{10}/MWCNTs	337.5	1.4
Pt_{25}/MWCNTs	509.3	2.3
Pt_{25}/C-Vulcan	361.1	1.8

*calculated with $Q_{Pt} = 210\mu C\ cm^{-2}$

A mechanism of reduction of NO^{3-} in alkaline medium per the studies (Nicholson *et al*., 1964; 1965; Manzo-Robledo *et al*., 2007), in which in accordance tendency of the reduction potentials peaks, we would have as main product is favored to N_2 and ammonium in alkaline medium, using platinum and boron-doped diamond electrodes, complementing with a sequence proposed by Estudillo-Wong *et al*. (2011), since the reduction of NO^{3-} to N_2 species using a Pt supported on carbon electrocatalyst in basic medium, are shown in the eqs. (2)-(6), it is also presented the generation and adsorption of species $H^*_{(ads)}$ to the production of hydrogen eq. (7), although these reactions would be confirmed with analysis techniques as mass spectrum, in order to obtain an overall reduction process.

$$NO^-_{3(ads)} + H_2O + 2e^- \longrightarrow NO^-_{2(aq)} + 2OH^- \quad (2)$$

$$2NO^-_{3(ads)} + 3H_2O + 10e^- \longrightarrow N_{2(g)} + 6OH^- \quad (2')$$

$$NO^-_{2(ads)} + H_2O + e^- \longrightarrow NO_{(aq)} + 2OH^- \quad (3)$$

$$2NO^-_{2(ads)} + 4H_2O + 6e^- \longrightarrow N_{2(g)} + 8OH^- \quad (3')$$

$$NO_{(ads)} + H_2O + e^- \longrightarrow HNO_{(aq)} + 2OH^- \quad (4)$$

$$2HNO_{(ads)} \longrightarrow N_2O_{(ads)} + 6OH^- \quad (5)$$

$$N_2O_{(ads)} + H_2O + 2e^- \longrightarrow N_{2(g)} + 2OH^- \quad (6)$$

$$2H_2O + 2e^- \longrightarrow 2H^+ + 2OH^- \longrightarrow (H* + H*)_{ads} + 2OH^- \longrightarrow H_2 + 2OH^- \quad (7)$$

The previous reactions imply an electronic or multielectronic transfer (except eq. (5), pure chemical reaction), as well as the adsorption of nitrated and OH^- species on the surface of the electrode, are important aspects that can affect the kinetics of the reaction, so the support is an important component of the electrocatalyst to facilitate an electronic transfer to certain products. The nitrate electro-reduction reaction in the eqs. (2') and (3') could be carried out directly to N_2 in a multielectronic process, this selective catalytic reduction is fully desired (Brylev *et al*., 2007).

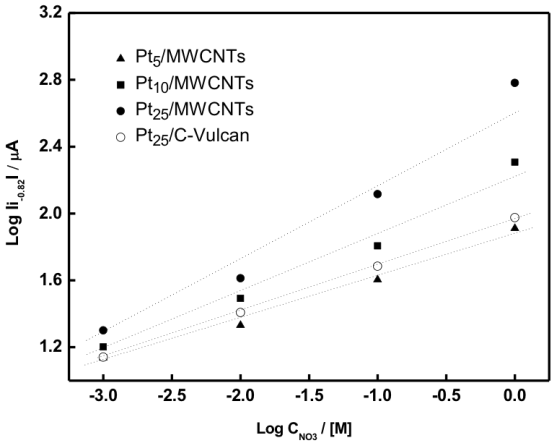

Fig. 5. Logarithmic plots of the nitrate reduction current ($i_{-0.82}$) as a function of the nitrate concentration.

Fig. 5 shows the logarithmic plots of the nitrate reduction current ($i_{-0.82}$) as a function of the nitrate concentration. Current was estimated at -0.82 V/SCE, close to i_p, where pure kinetic phenomena are taking place, because the rate reaction at the electrode-electrolyte interface at this point is controlled by the transfer of electrons and not determined by the mass transport (Srinivasan, 2006). The data linear approximation yields a slope corresponding to the order of the reaction associated to the reduction reaction in accordance to eq. (8):

$$\log|i_{-0.82}| = \log kf + \beta \log[NO_3^-] \qquad (8)$$

where β is the reaction order and kf is the rate constant (Reyter *et al*., 2006). Both Pt/MWCNTs and Pt/C-Vulcan present reaction orders lower than 1 (Table 3), where the value obtained for the support C-Vulcan is similar in accordance to reported in other study of reference (Estudillo-Wong *et al*., 2011).

Table 3. Reaction order β and reaction rate constant k_f for Pt/MWCNTs and Pt/C-Vulcan

Electrocatalyst	β*	k_f μA [mol L^{-1}]$^{-\beta}$
Pt_5/MWCNTs	0.22	52.26
Pt_{10}/MWCNTs	0.36	173.78
Pt_{25}/MWCNTs	0.49	489.77
Pt_{25}/C-Vulcan	0.25	75.86

*calculated at E = -820 mV / SCE

The values founded in this study probably indicate that not only the nitrate concentration influences the reduction, but also the intrinsic favorable features of MWCNTs as structural and electronic, suggests that they have the ability to promote electrons transfer reaction when used as an electrode material (Capula-Colindres *et al*., 2019), allowing to have better values in the NER activity (Weihua *et al*. 2008). The considerable high rate constants for Pt/MWCNTs are consistent with the high catalytic activity.

Conclusions

Pt nanoparticles were supported on MWCNTs and C-Vulcan XC72 by a vapor-phase impregnation-decomposition method and their catalytic activity was investigated in the NER process. Both types of carbon support and the particle incorporation method favor the formation and dispersion of small Pt particles. The NER showed superior activity with Pt/MWCNTs materials than Pt/C-Vulcan XC72, even when both catalysts are comparable in ECSA, particle size, distribution and content of Pt on the conventional carbon support. The superior nitrate electroreduction activity was associated to the inherent structural and electronic features of MWCNTs. Optimum content of Pt supported on MWCNTs was 25 wt.% according to the results of current reduction nitrate, reaction order β and rate constant kf. Thus, Pt/MWCNTs are attractive materials for electrodes on the nitrate reduction process in alkaline medium.

Acknowledgements

This investigation was supported by the scholarship received from the National Council of Science and Technology (CONACyT).

References

Abbasi S., Seyed M. Z., Seyed H., Noie B. (2013). Decorating and filling of multi-walled carbon nanotubes with TiO_2 nanoparticles via wet chemical method. *Engineering 5*, 207-212. https://file.scirp.org/pdf/ENG_2013021809013480.pdf

Bahman R., Sayed B. M., Gholamreza M., Dariush R.V., Soleyman M. (2011). Experimental

investigation of the chemical reduction of nitrate in water by MgO and Cu/Mg bimetallic particles in the absence of any pH-control mechanism. *Fresenius Environmental Bulletin 20*, 2475-2484.

Baughman R. H., Zakhidov A. A., Heer W. A. (2002). Carbon nanotubes-the route toward applications. *Science 297*, 787-792. http://science.sciencemag.org/content/297/5582/787.

Bhatnagar A, Kumar E, Sillanpää M. (2010). Nitrate removal from water by nano-alumina: characterization and sorption studies. *Chemical Engineering Journal 163*, 317-323.

Brylev O., Sarrazin M., Bélanger D., Roué L. (2007). Nitrate and nitrite electrocatalytic reduction on Rh-modified pyrolytic graphite electrodes. *Electrochimica Acta 52*, 6237-6247.

Capula Colindres S., Vargas J.R., Toledo J.A., Angeles Chavez C. (2009). Preparation of platinum-iridium nanoparticles on titania nanotubes by MOCVD and their catalytic evaluation. *Journal of Alloys and Compounds 483*, 406-409. https://doi.org/10.1016/j.jallcom.2008.08.097.

Capula-Colindres S., Terán G., Torres-Santillan E., Villa-Vargas L., Velázquez J.C. (2019). Dispersion of carbon nanotubes and their influence for ozone monitoring. *Revista Mexicana de Ingeniería Química 18*, 143-150.

Couto A.B., Oishi S.S., Ferreira N.G. (2016). Enhancement of nitrate electroreduction using BDD anode and metal modified carbon fiber cathode. *Journal of Industrial and Engineering Chemistry 39*, 210-217.

Cheng J. P., Zhang X. B., Yi G. F., Ye Y., Xia M.S. (2008). Preparation and magnetic properties of iron oxide and carbide nanoparticles in carbon nanotube matrix. *Journal of Alloys and Compounds 455*, 5-9.

Encarnacion C., Vargas J. R., Toledo J. A., Cortes J. C., Angeles M. A. (2010). Pt nanoparticles on titania nanotubes prepared by vapor-phase impregnation decomposition method. *Journal of Alloys and Compounds 495*, 458-461.

Estudillo-Wong L. A., Alonso-Vante N., Manzo-Robledo A. (2008). Electro-reduction of nitrate and nitrite ions on carbon-supported Pt nanoparticles. *ECS Transactions 15*, 385-393. doi: 10.1149/1.3046654

Estudillo-Wong L.A., Arce-Estrada E.M., Alonso-Vante N., Manzo-Robledo A. (2011). Electro-reduction of nitrate species on Pt-based nanoparticles: Surface area effects. *Catalysis Today 166*, 201-204.

Fanning J. C. (2000). The chemical reduction of nitrate in aqueous solution. *Coordination Chemistry Reviews 199*, 159-179.

Groot M.T. de, Koper M.T.M. (2004). The influence of nitrate concentration and acidity on the electrocatalytic reduction of nitrate on platinum. *Journal of Electroanalytical Chemistry 562*, 81.

Halder A., Sharma S., Hegde M. S, Ravishankar N. (2009). Controlled attachment of ultrafine platinum nanoparticles on functionalized carbon nanotubes with high electrocatalytic activity for methanol oxidation. *Journal of Physical Chemistry C 113*, 1466-1473.

Hernández-Fydrych V.C., Castilla-Hernández P., Beristain-Cardoso R., Trejo-Aguilar, G.M., Fajardo-Ortiz C. (2018). COD and ammonium removal in SBR operated under different combinations using pre-treated slaughterhouse wastewater. *Revista Mexicana de Ingeniería Química 17*, 621-631.

Kerkeni S., Lamy-Pitara E., *et al*., (2002). Copper-platinum catalysts prepared and characterized by electrochemical methods for the reduction of nitrate and nitrite. *Catalysis Today 75*, 35-42.

Kijima, Shimizu H., Takasawa Y., Nakamura. (2004). Efficient usage of highly dispersed Pt on carbon nanotubes for electrode catalysts of polymer electrolyte fuel cells. *Catalysis Today 90*, 277-281.

Lehman S. G., Badruzzaman M., Adham S., Roberts D. J. Clifford D. A. (2008). Perchlorate and nitrate treatment by ion exchange integrated with biological brine treatment. *Water Research 42*, 969-976. https://doi.org/10.1016/j.watres.2007.09.011

Lim B.K., Jiang M. Camargo P.H.C., Cho E.C., Tao J., Lu X., Zhu Y., Xia Y. (2009). Pd-Pt bimetallic nanodendrites with high activity for oxygen reduction. *Science 324*, 1302-1305.

Luk G.K., Au-Yeung W.C. (2002). Stability and quality of municipal solid waste compost from a landfill aerobic bioreduction process. *Advances of Environmental Research 6*, 441-453.

Martínez J., Ortiz A., Ortiz I. (2017). State-of-the-art and perspectives of the catalytic and electrocatalytic reduction of aqueous nitrates. *Applied Catalysis B: Environmental 207*, 42-59. https://doi.org/10.1016/j.apcatb.2017.02.016

Manzo-Robledo A., Levy-Clement A.C., Alonso-Vante N. (2007). Electrochemical behavior of nitrogen gas species adsorbed onto Boron-Doped Diamond (BDD) electrodes. *Langmuir 23*, 11413-11416.

Mercado-Zuñiga C., Vargas-Garcia J.R., Hernandez-Perez M.A., Figueroa-Torres M.Z., Cervantes-Sodi F., Torres-Martínez L.M. (2014). Synthesis of highly dispersed platinum particles on carbon nanotubes by an in-situ vapor-phase method. *Journal of Alloys and Compounds 106*, 406-409.

Nicholson R. S., Shain I. (1964). Theory of stationary electrode polarography. Single scan cyclic methods applied to reversible, irreversible, and kinectic systems. *Analytical Chemistry 36*, 706-723.

Nicholson R. S., Shain I. (1965). Theory of stationary electrode polarography for a chemical reaction coupled between tow charge transfer. *Analytical Chemistry 37*, 178-190.

Park H. I., Kim D. K., Choi Y. J., D- Pack. (2005). Effect of nitrate on the performance of single chamber air cathode microbial fuel cells. *Process Biochemistry 40*, 3383-3388.

Patel A., Zuo G., et. al. (2008). Fluidized bed reactor for the biological treatment of ion-exchange brine containing perchlorate and nitrate. *Water Research 42*, 4291.

Prusse U., Hahnlein M., Daum J., Vorlop K.-D. (2000). Improving the catalytic nitrate reduction. *Catalysis Today 55*, 79-90.

Reyter D., Chamoulaud G., Bélanger D., Roué L. (2006). Electrocatalytic reduction of nitrate on copper electrodes prepared by high-energy ball milling. *Journal of Electroanalytical Chemistry 596*, 13-24.

Serp P., Corrias M., Kalck P. (2003). Carbon nanotubes and nanofibers in catalysis. *Applied of Catalysis A-Gen. 253*, 337-358. https://doi.org/10.1016/S0926-860X(03)00549-0

Schoeman J. J., Steyn. A. (2003). Nitrate removal with reverse osmosis in a rural area in South Africa. *Desalination 155*, 15-26.

Shenga X., Benny W., Tom B., Annick H., Vankelecoma F.J., Paolo P. P. (2014). Cu/CuxO and Pt nanoparticles supported on multi-walled carbon nanotubes as electrocatalysts for the reduction of nitrobenzene. *Applied Catalysis B: Environmental 147*, 330-339.

Soares O. S. G. P., Orfao J.J.M., Pereira M. F. R. (2011). Pd−Cu and Pt−Cu Catalysts Supported on Carbon Nanotubes for Nitrate Reduction in Water. *Desalination 279*, 367-374.

Srinivasan S. (2006). *Fuel Cells: From Fundamentals to Applications*. Springer Science.

Taguchi S., Feliu J.M., (2008), Kinetic study of nitrate reduction on Pt (110) electrode in perchloric acid solutions. *Electrochimica Acta 53*, 3626-3634.

Toma F. L., Bertrand G., Chwa S. O., Meunier C., Klein D., Coddet C. (2006). Comparative study on the photocatalytic decomposition of nitrogen oxides using TiO_2 coatings prepared by conventional plasma spraying and suspension plasma spraying. *Surface and Coatings Technology 200*, 5855-5862.

Torres-Santillan E., Capula-Colindres S., Reza-San German C.M., Cayetano-Castro N., Villagarcia-Chavez E. (2018). Effect of functional groups in the structure of carbon nanotubes to adsorption grade of cadmium ions. *Revista Mexicana de Ingeniería Química 17*, 955-961.

Trépanier M., Tavasoli A., Dalai A.K., Abatzoglou N. (2009). Fischer-Tropsch synthesis over carbon nanotubes supported cobalt catalysts in a fixed bed reactor: Influence of acid treatment. *Fuel Processing Technology 90*, 367-374.

Vahlas C., Caussat B., Serp P., Angelopoulos G. N. (2006). Principles and applications of CVD powder technology. *Materials Science and Engineering R 53*, 1-72.

Wang Y., Kmiya Y., Okuhara T. (2007). Removal of low concentration ammonia in water by ion-exchange using Na-mordenite. *Water Research 41*, 269-276. https://doi.org/10.1016/j.watres.2006.10.035

Wang Y., Qu J., Wu R., Lei P. (2006). The electrocatalytic reduction of nitrate in water on Pd/Sn-modified activated carbon fiber electrode. *Water Research 40*, 1224-1232.

Weihua G, Lin X., Bingbing X., Yanyan Y., Zhixia S., Shuping L. (2008). A modified composite film electrode of polyoxometalate/carbon nanotubes and its electrocatalytic reduction. *Journal of Applied Electrochemistry 39*, 647-652.

Xiaomeng F., Xiaohong G., Jun M., Hengyu A. (2009), Kinetics and corrosion products of aqueous nitrate reduction by iron powder without reaction conditions control. *Journal of Environmental Sciences 21*, 8, 1028-1035.